

FEATURE DENOISING FOR LOW-LIGHT INSTANCE SEGMENTATION USING WEIGHTED NON-LOCAL BLOCKS

Joanne Lin, Nantheera Anantrasirichai and David Bull

Visual Information Laboratory, University of Bristol

ABSTRACT

Instance segmentation for low-light imagery remains largely unexplored due to the challenges imposed by such conditions, for example shot noise due to low photon count, color distortions and reduced contrast. In this paper, we propose an end-to-end solution to address this challenging task. Based on Mask R-CNN, our proposed method implements weighted non-local (NL) blocks in the feature extractor. This integration enables an inherent denoising process at the feature level. As a result, our method eliminates the need for aligned ground truth images during training, thus supporting training on real-world low-light datasets. We introduce additional learnable weights at each layer in order to enhance the network’s adaptability to real-world noise characteristics, which affect different feature scales in different ways. Experimental results show that the proposed method outperforms the pretrained Mask R-CNN with an Average Precision (AP) improvement of **+10.0**, with the introduction of weighted NL Blocks further enhancing AP by **+1.0**.

Index Terms— Instance segmentation, low-light images, feature denoising, non-local means, end-to-end

1. INTRODUCTION

Instance segmentation is a crucial task in computer vision because it allows systems to interpret scenes with higher levels of detail, by understanding the position and shape of the objects within them. This can be highly beneficial in scenarios such as autonomous driving, video surveillance, augmented reality, multimedia editing, medical imaging and agricultural monitoring. Its importance is underscored by numerous recent research contributions in this field and various benchmarks and datasets, including Microsoft COCO [1], ADE20K [2], Pascal VOC [3] and Cityscapes [4].

While its applications span many sectors, there has been limited research on instance segmentation in low-light conditions. This is due to the fact that low-light images are heavily affected by noise from a low photon count in darker conditions, making the task much more challenging. A common approach is to first apply a low-light image enhancement

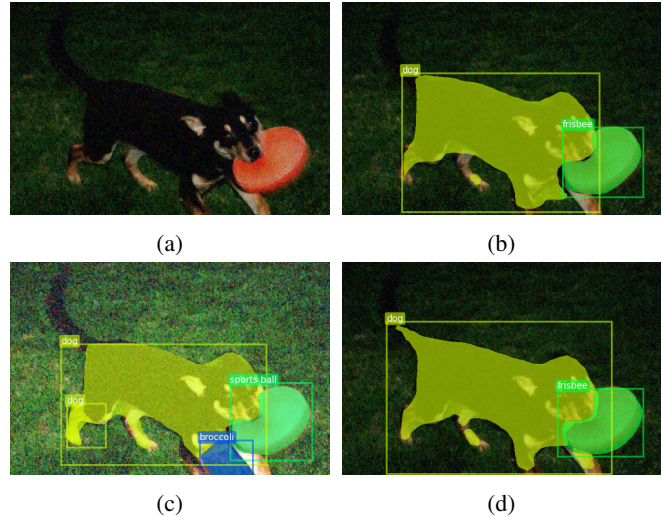


Fig. 1: Results of applying instance segmentation to (a) a low-light image using (b) a pretrained Mask R-CNN model [5], (c) a RetinexFormer [6] for LLIE, and (d) our method.

(LLIE) method to these images. This enables existing instance segmentation methods, typically designed for normal-light conditions, to run inference upon the enhanced images. LLIE methods include EnlightenGAN [7], Zero-DCE [8], and more recently RetinexFormer [6]. Specifically, Zero-DCE [8], and RetinexFormer [6] also use low-light object detection benchmarks (ExDark [9], DARK FACE [10]) to show their low-light enhancing performances.

To the best of our knowledge to date, the only work published on low light instance segmentation is by by Chen et al. [11]; however their method was only applicable for RAW images to take advantage of the higher bit-depth. In this paper, we propose an end-to-end approach that takes low-light sRGB images as inputs; these are much more widely used than RAW images and can be applied to video sequences.

Our goal is to develop a robust and effective end-to-end method for low-light instance segmentation. This implies eliminating any explicit pre-processing steps in order to simplify the mask generating procedure. However most models are not designed to handle images with noise and low-contrast. In our experiments, we have found that both

This work was supported by UKRI MyWorld Strength in Places Programme (SIPF00006/1)

low-contrast and noise impact the performance of these models, as also confirmed by the study in [12].

Our focus is to build upon existing feature extractors to learn to ignore the presence of noise in the feature maps. This is achieved by integrating denoising blocks with non-local (NL) means as its denoising operation into the backbone. Specifically, our framework is based on Mask R-CNN [5] and leverages an NL block [13] for denoising in the feature extractor. We however extend this with a weighted NL block, where the additional learnable weights ensure that the network can learn the noise characteristics that affect each scale of feature space differently. We trained our framework with a synthetic dataset; this is due to the infancy of performing high-level computer vision tasks under low-light conditions. We used the popular Microsoft COCO [1] dataset and synthesised low-light conditions following the pipeline proposed by [14].

2. RELATED WORK

2.1. Instance Segmentation

Instance segmentation aims to produce a segmentation mask, bounding box and class label for every object detected in an image. One of the most popular techniques for achieving this is Mask R-CNN [5], introduced by He et al. as an extension to the popular object detection model, Faster R-CNN [15]. The architecture is the same except Mask R-CNN [5] introduced a new mask head to also predict the instance masks from the Regions of Interest (RoIs) proposed by the Region Proposal Network (RPN). With the notable work from [16], there has been a surge in transformer-based methods in recent years. For example, DETR-based [17] instance segmentation methods use CNN-based feature extraction backbones and concatenate positional embeddings before passing into a transformer.

2.2. Low-light image enhancement

Traditional LLIE methods treat the problem as two separate tasks: contrast enhancement and denoising. Contrast enhancement methods include gamma correction and adaptive histogram equalization (AHE) [18]; however these lack consideration of illumination factors, leading to cognition approaches inspired by Retinex Theory [19]. Contrast-enhancement of low-light images however, amplifies noise which necessitates the use of denoising algorithms for further refinement.

Recent advancements in LLIE have explored the use of deep learning. Lore et al. first introduced LLNet [20], an autoencoder trained with synthetic low-light images. Supervised methods, including RetinexNet [21], KiND [22], and AGLNet [14], require large sets of paired normal/low-light images for training, often generated synthetically. Unsupervised methods gained popularity due to the scarcity of paired

normal-light images in low-light datasets. Examples include EnlightenGAN [7] and Zero-DCE (and its extended version Zero-DCE++) [8]. RetinexFormer [6], a transformer-based method, is currently the state-of-the-art approach, leveraging the Retinex theory [19] to separate color vision into reflectance and luminance components.

2.3. Low-light scene understanding

Several datasets have been released for higher computer vision tasks in low-light conditions. Semantic segmentation is a more common task, with datasets like NightCity [23] and BDD100K-night [24] focusing on analyzing road scenes to enhance autonomous driving at night. Additionally datasets such as ExDark [9] and DARK FACE [10] serve as benchmarks for low-light object detection.

Chen et al. [11] investigated instance segmentation in extreme low-light conditions, leveraging the higher bit-depth of RAW images to enhance scene parsing. Their approach introduces three key contributions: an adaptive weighted downsampling (AWD) layer incorporating spatial and channel information for downsampling, a smooth-oriented convolutional block replacing standard 3×3 convolutions during training and re-parameterizing back into a 3×3 convolution block, and a disturbance suppression loss (DSL) measuring Euclidean distance between feature maps from clean and noisy images. Training involves the synthesis of both a clean RAW low-light dataset and a noisy RAW low-light dataset for the disturbance suppression loss. They provided a low-light dataset with paired short-exposure/long-exposure images for instance segmentation training and validation.

3. SYNTHETIC LOW-LIGHT PIPELINE

For training and evaluating our method, we require annotated low-light images for instance segmentation. However, to the best of our knowledge, there currently exists only one small dataset, released by Chen et al. [11]. This real-world low-light dataset however contains only 2230 paired short-exposure/long-exposure images with instance-level segmentation annotations. Due to the limited number of training paired samples with imagery only in extreme low-light conditions, we decided not to use this dataset. Instead we chose to synthetically create an annotated low-light dataset.

We used the popular Microsoft COCO [1] dataset and passed it through the synthetic low-light pipeline proposed by Lv et al. [14]. This method was chosen over a simplified model (e.g. [25]) because of the simulated in-camera processing which also factors in spatial correlations of noise caused by demosaicing thereby generating more realistic noise characteristics.

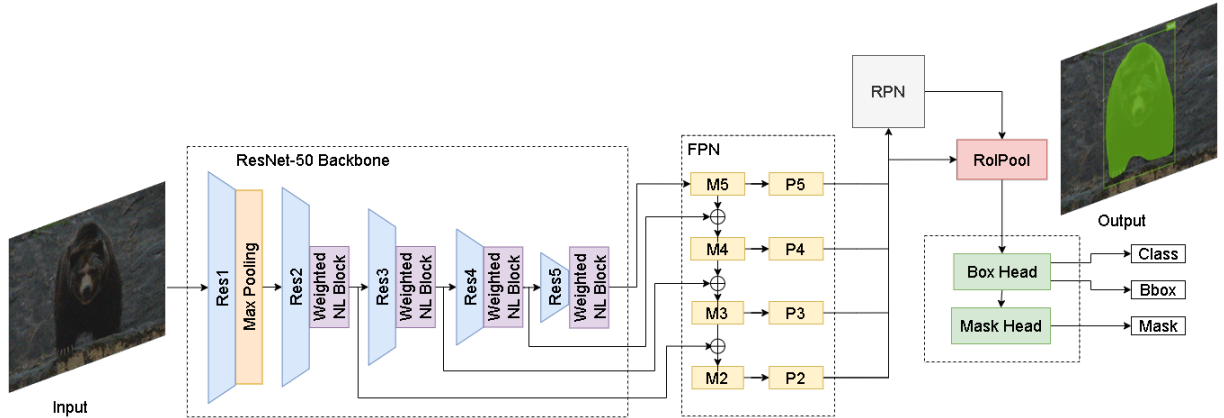


Fig. 2: Proposed architecture inspired by Mask R-CNN [5]. A weighted non-local (NL) block [13] used for feature denoising in the feature extractor. The extracted feature maps are passed into a Region Proposal Network (RPN) and Region of Interest (RoI) pooling layer to get the features for the proposed regions. These features are passed into the box and mask heads for predictions. The image used in this diagram was taken from the MS COCO dataset [1].

4. PROPOSED METHOD

4.1. Instance Segmentation

We propose an end-to-end method for instance segmentation in low-light without the need for paired normal-light images. Following the popular Mask R-CNN [5], the network is constructed of a backbone, a Region Proposal Network (RPN), Region of Interest (RoI) pooling, and box and mask heads.

The image is first passed into the modified backbone to extract features. The feature maps are then passed into the RPN first introduced by [15] to generate object proposals with a objectiveness score. These proposals and the feature maps are passed into the RoIPool layer which extracts the feature maps within the proposals. These RoIs are then passed into the box head and mask head to make predictions on the class, bounding box and segmentation mask for each RoI.

For our backbone, we chose to use ResNet-50 [26] with a feature pyramid network (FPN) [27]; this is a popular backbone capable of learning features at different scales. We modify this backbone by adding our weighted NL blocks at the end of *res2*, *res3*, *res4* and *res5* to reduce the feature noise that has been propagated into the feature extractor. The remainder of the network uses the originally proposed parameters from Mask R-CNN [5]. For training, we froze the weights of everything except the backbone to allow the model to specifically learn to denoise the feature maps.

4.2. Weighted non-local blocks for feature denoising

Traditional non-local blocks were first introduced by Wang et al. [13] when they explored implementing non-local means into neural networks. Non-local means [28] is a class of traditional computer vision denoising algorithm that process images on a global scale, unlike local smoothing filters (e.g. bi-

lateral filter [29], Gaussian filter etc.) which only consider neighbouring pixels. Non-local means filtering involves calculating the mean of all pixels in the image, with the weighting determined by the similarity of each pixel to the target one. Wang et al. [13] applied this idea in their neural networks to learn long-range dependencies between pixels spatially and temporally. They also found that the self-attention mechanism [16] is a special form of NL operations in the embedded gaussian form [13].

Xie et al. [30] explored using both non-local means algorithms and local smoothing filtering algorithms for feature denoising to defend against adversarial attacks; attacks that intentionally insert noise into images to confuse systems. They found that although the local denoising operations did improve the robustness of these systems, NL operations were more effective.

In this paper we consider three implementations of NL means for denoising: *dot product*, *Gaussian* and *embedded Gaussian*. The NL blocks consist of an implementation of non-local mean followed by a 1×1 convolution, added to the block's input via an identity skip connection. They achieve feature denoising as they pass the feature maps through a denoising operation (i.e. non-local means). We modified these blocks to include learnable weight w as shown in Fig. 3. This allows the model to determine the amount of denoising for each ResNet layer. We refer to it as a weighted NL block, which computes the following:

$$\mathbf{z} = wW_z\mathbf{y} + (1 - w)\mathbf{x} \quad (1)$$

where \mathbf{x} is the input feature map, \mathbf{y} is the output from the NL means operation, W_z is the weight matrix from the 1×1 convolutional layer after the NL means operation and \mathbf{z} is the output.

Table 1: Comparison of methods on the synthetic low-light COCO minival dataset

| Method | LLIE | AP | AP ₅₀ | AP ₇₅ | AP _S | AP _M | AP _L |
|---------------------------------|-------------------|-------------|------------------|------------------|-----------------|-----------------|-----------------|
| Pretrained | - | 6.9 | 12.4 | 6.9 | 2.3 | 7.4 | 12.4 |
| Pretrained | EnlightenGAN [7] | 5.5 | 10.0 | 5.5 | 1.7 | 6.1 | 10.0 |
| Pretrained | Zero-DCE++ [8] | 5.6 | 10.0 | 5.6 | 1.8 | 6.1 | 9.6 |
| Pretrained | AGLLNet [14] | 6.1 | 11.0 | 6.1 | 1.8 | 7.2 | 10.5 |
| Pretrained | RetinexFormer [6] | 5.7 | 10.3 | 5.7 | 1.8 | 6.5 | 9.9 |
| Finetuned | - | 15.9 | 28.6 | 15.6 | 4.8 | 15.8 | 27.8 |
| Ours (weighted non-local block) | - | 16.9 | 30.7 | 16.6 | 5.6 | 17.2 | 28.9 |

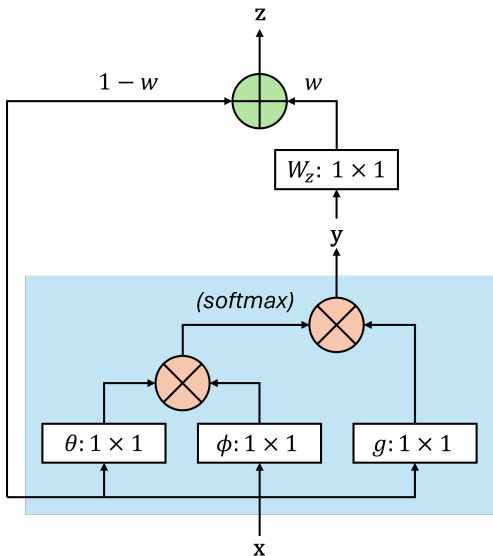


Fig. 3: A weighted non-local block for feature denoising with learnable weight w . The blue box illustrates the non-local operation used for denoising an input feature map x . This figure shows the embedded Gaussian form.

5. EXPERIMENTAL RESULTS

For all of our experiments, we trained the models for 10 epochs with an initial learning rate of 0.0005 that decreased by a factor of 10 every 3 epochs, with a batch size of 4. Due to limited computational resources, the number of channels inside the weighted NL block after *res2* were divided into 4 instead of 2 as proposed originally by Wang et al. [13]. We used the Microsoft COCO [1] dataset and ran it through the low-light synthetic pipeline. We used 118,287 images for training and 5,000 for evaluation. We did not use their test set as it does not have public annotations available. We used the metrics provided by MS COCO: AP, AP₅₀, AP₇₅, AP_S, AP_M, and AP_L. AP calculates the mean of the average precisions across multiple IoU thresholds, 0.5 to 0.95, in 0.05 increments. AP₅₀ and AP₇₅ calculate the average precision with an IoU threshold of 0.5 and 0.75 respectively. AP_S,

AP_M, and AP_L calculate the average precision for small, medium and large objects, which are predefined by [1].

Table 1 shows our results compared to several different methods based around Mask R-CNN [5]. We experimented with one-stage methods and two-stage methods (using LLIE methods [8, 7, 14, 6] for the pre-processing step). We did not run our experiments with a weighted non-local block on *res2* due to memory limitations.

5.1. One-stage experiments

Our baseline experiments compare our proposed method with a pretrained Mask R-CNN model [5] and also with finetuning the pretrained model on synthetic low-light training data generated from [1]. Table 1 shows a significant improvement between the fine-tuned model and the pre-trained model. Additionally, there is further enhancement when the weighted NL blocks are integrated, resulting in a **+1.0** AP improvement.

Both Table 1 and Fig. 4 illustrate the efficacy of our method in enhancing performance, while also indicating areas for further refinement. Generally, the models exhibit proficiency in segmenting larger objects but encounter challenges with smaller ones, likely attributed to injected noise. The *easy* example case in Fig. 4 had one large object of a cat and all models were able to accurately generate an instance mask for it. In the *medium* case, the pretrained Mask R-CNN method failed significantly and falsely labelled many pixels due to the low-light conditions. The finetuned Mask R-CNN performed better although it still suffered with accuracy when segmenting the tennis racket, while our method did not have this issue. In the *difficult* case, there are small cows in the distance but none of the methods were able to pick them up. These findings are backed by the results from Table 1, particularly the metrics AP_S, AP_M and AP_L. These metrics clearly show that our method improves on the finetuned method for different sized objects, indicating that the weighted NL block successfully removes the noise in the feature extractor.

5.2. Two-stage experiments

We also compared our method with the two-stage approaches, where the pre-processing employed popular LLIE methods,

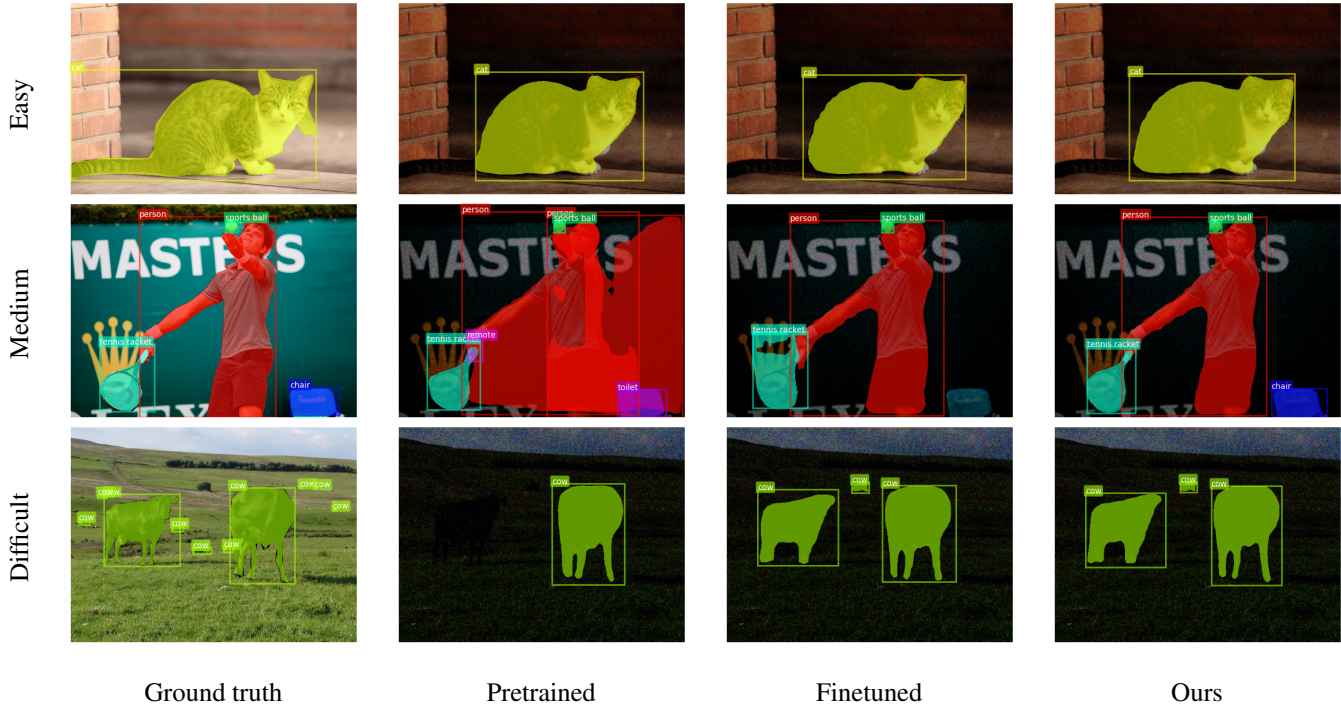


Fig. 4: Visual comparison of our proposed method against pretrained and finetuned Mask R-CNN [5] models, along with the ground truth, with varying levels of difficulty for the models. The *easy* example case shows when these methods were all successful. The *medium* example case shows when our proposed method performed successfully while the other two methods failed. The *difficult* example case shows when all of the methods struggle. The images used in this diagram were taken from the MS COCO dataset [1].

including EnlightenGAN [7], Zero-DCE++ [8], AGLNet [14], and RetinexFormer [6]. All of these methods used the weights released by them (for RetinexFormer, we used the weights trained from the LOL [21] dataset). It can be seen from Table 1 that these approaches underperformed compared to using a pretrained model, primarily because the enhanced images were significantly impacted by noise (see Fig. 5, even with the transformer-based method RetinexFormer which reformulated the equation from the Retinex theory to also model noise and reduce the noise amplification. In the example shown, the two-stage methods unsuccessfully generated masks for the giraffe. We found that, of all of the LLIE methods used, AGLNet performed the best. This may be because their model was trained with the synthetic data generated using the same synthetic low-light pipeline as ours.

5.3. Ablation study

We compared our approach with using different NL operations in order to determine which was the most effective method. As seen in Table 2, they all show similar performances, but the embedded Gaussian form shows some improvement compared to the other two. The embedded Gaussian form likely had a higher performance due to its self-

attention properties, as described by Wang et al. [13].

Table 2: Ablation study of different NL operations for NL block with weights $w_1 = 0$, $w_2 = 0$, $w_3 = 0.5$, $w_4 = 0$

| Method | AP | AP ₅₀ | AP ₇₅ |
|-------------------|-------------|------------------|------------------|
| Dot Product | 16.1 | 29.3 | 15.7 |
| Gaussian | 16.0 | 29.1 | 15.7 |
| Embedded Gaussian | 16.6 | 30.2 | 16.4 |

6. CONCLUSION

This paper introduces a framework for low-light instance segmentation without the need for pre-processing. We enhance popular instance segmentation models by proposing a weighted non-local block for feature denoising, improving performance for smaller objects that would previously most likely be obscured by noise. Experimental results show that our method improves the average precision by **+10.0** over a vanilla pretrained Mask R-CNN. Our approach is applicable to various low-light computer vision tasks, including object detection and semantic segmentation, by integrating

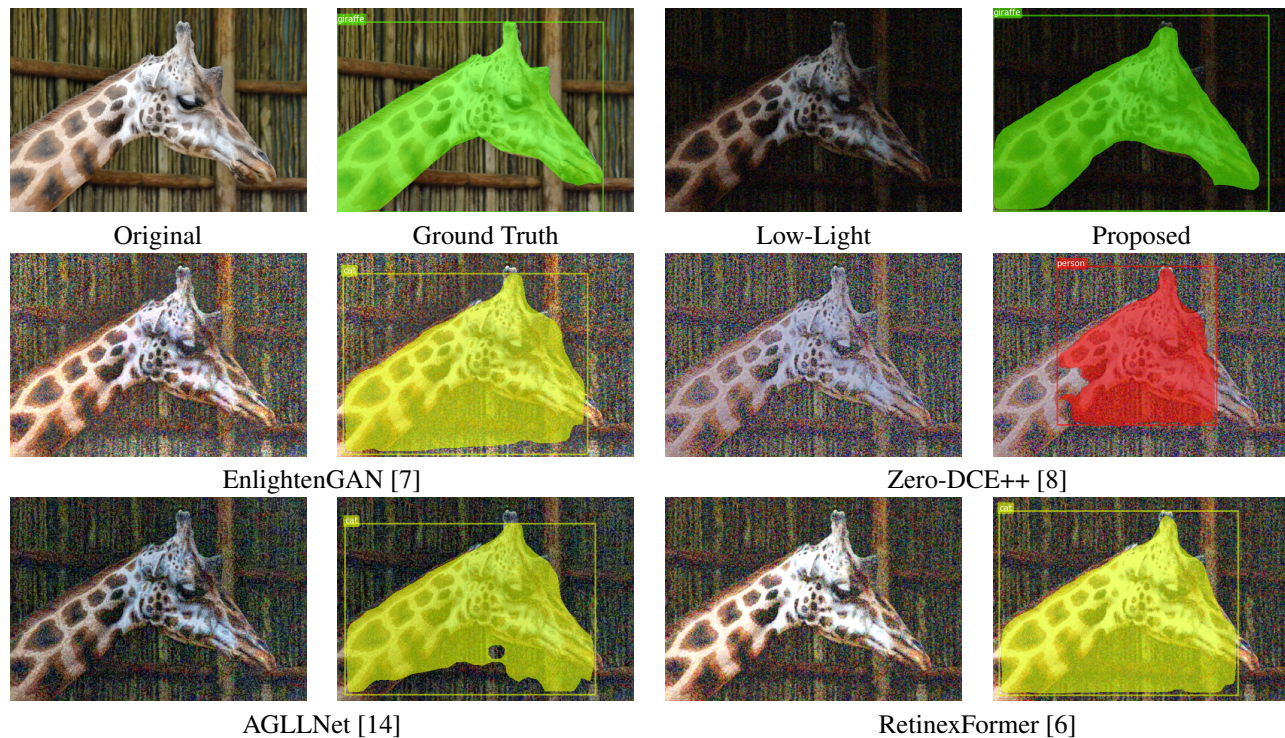


Fig. 5: Visual comparison of our proposed method against two-stage methods (enhanced first then passed through a pretrained Mask R-CNN [5]). The first row shows the original image with the ground truth annotations, and the low-light image with predictions from our proposed method. The second and third row shows the enhanced images and the predictions using a pretrained Mask R-CNN [5]. The image used in this diagram was taken from the MS COCO dataset [1].

weighted NL blocks into the backbones of other architectures. Future work should address performance on even smaller objects, enhance other aspects such as the FPN, and assess our method’s efficacy on real low-light datasets.

7. REFERENCES

- [1] Tsung-Yi Lin, Michael Maire, Serge Belongie, James Hays, Pietro Perona, Deva Ramanan, Piotr Dollár, and C Lawrence Zitnick, “Microsoft coco: Common objects in context,” in *European Conference on Computer Vision*, 2014, pp. 740–755.
- [2] Bolei Zhou, Hang Zhao, Xavier Puig, Sanja Fidler, Adela Barriuso, and Antonio Torralba, “Scene parsing through ade20k dataset,” in *Proceedings of the IEEE Conference on Computer Vision and Pattern Recognition*, 2017.
- [3] M. Everingham, S. M. A. Eslami, L. Van Gool, C. K. I. Williams, J. Winn, and A. Zisserman, “The pascal visual object classes challenge: A retrospective,” *International Journal of Computer Vision*, vol. 111, no. 1, pp. 98–136, Jan. 2015.
- [4] Marius Cordts, Mohamed Omran, Sebastian Ramos, Timo Rehfeld, Markus Enzweiler, et al., “The cityscapes dataset for semantic urban scene understanding,” in *Proceedings of the IEEE Conference on Computer Vision and Pattern Recognition (CVPR)*, June 2016.
- [5] Kaiming He, Georgia Gkioxari, Piotr Dollár, and Ross Girshick, “Mask r-cnn,” in *2017 IEEE International Conference on Computer Vision (ICCV)*, 2017, pp. 2980–2988.
- [6] Yuanhao Cai, Hao Bian, Jing Lin, Haoqian Wang, Radu Timofte, and Yulun Zhang, “Retinexformer: One-stage retinex-based transformer for low-light image enhancement,” in *Proceedings of the IEEE/CVF International Conference on Computer Vision (ICCV)*, October 2023, pp. 12504–12513.
- [7] Yifan Jiang, Xinyu Gong, Ding Liu, Yu Cheng, Chen Fang, Xiaohui Shen, Jianchao Yang, Pan Zhou, and Zhangyang Wang, “Enlightengan: Deep light enhancement without paired supervision,” *IEEE Transactions on Image Processing*, vol. 30, pp. 2340–2349, 2021.
- [8] Chongyi Li, Chunle Guo Guo, and Chen Change Loy, “Learning to enhance low-light image via zero-reference deep curve estimation,” in *IEEE Transactions on Pattern Analysis and Machine Intelligence*, 2021.
- [9] Yuen Peng Loh and Chee Seng Chan, “Getting to know low-light images with the exclusively dark dataset,” *Computer Vision and Image Understanding*, vol. 178, pp. 30–42, 2019.
- [10] Wenhan Yang, Ye Yuan, Wenqi Ren, Jiaying Liu, Walter J. Scheirer, et al., “Advancing image understanding in poor visibility environments: A collective benchmark study,” *IEEE Transactions on Image Processing*, vol. 29, pp. 5737–5752, 2020.

- [11] Linwei Chen, Ying Fu, Kaixuan Wei, Dezhi Zheng, and Felix Heide, "Instance segmentation in the dark," *International Journal of Computer Vision*, vol. 131, no. 8, pp. 2198–2218, 2023.
- [12] Anqi Yi and Nantheera Anantrasirichai, "A comprehensive study of object tracking in low-light environments," *arXiv:2312.16250*, 2024.
- [13] Xiaolong Wang, Ross Girshick, Abhinav Gupta, and Kaiming He, "Non-local neural networks," in *Proceedings of the IEEE Conference on Computer Vision and Pattern Recognition (CVPR)*, June 2018.
- [14] Feifan Lv, Yu Li, and Feng Lu, "Attention guided low-light image enhancement with a large scale low-light simulation dataset," *International Journal of Computer Vision*, vol. 129, no. 7, pp. 2175–2193, 2021.
- [15] Shaoqing Ren, Kaiming He, Ross Girshick, and Jian Sun, "Faster r-cnn: Towards real-time object detection with region proposal networks," in *Advances in Neural Information Processing Systems*, 2015, vol. 28.
- [16] Ashish Vaswani, Noam Shazeer, Niki Parmar, Jakob Uszkoreit, Llion Jones, et al., "Attention is all you need," in *Advances in Neural Information Processing Systems*, 2017, vol. 30.
- [17] Nicolas Carion, Francisco Massa, Gabriel Synnaeve, Nicolas Usunier, Alexander Kirillov, and Sergey Zagoruyko, "End-to-end object detection with transformers," in *European conference on computer vision*. Springer, 2020, pp. 213–229.
- [18] Stephen M. Pizer, E. Philip Amburn, John D. Austin, Robert Cromartie, Ari Geselowitz, et al., "Adaptive histogram equalization and its variations," *Computer Vision, Graphics, and Image Processing*, vol. 39, no. 3, pp. 355–368, 1987.
- [19] Edwin H Land, "The retinex theory of color vision," *Scientific american*, vol. 237, no. 6, pp. 108–129, 1977.
- [20] Kin Gwn Lore, Adedotun Akintayo, and Soumik Sarkar, "L-net: A deep autoencoder approach to natural low-light image enhancement," *Pattern Recognition*, vol. 61, pp. 650–662, 2017.
- [21] Chen Wei, Wenjing Wang, Wenhan Yang, and Jiaying Liu, "Deep retinex decomposition for low-light enhancement," in *British Machine Vision Conference*, 2018.
- [22] Yonghua Zhang, Jiawan Zhang, and Xiaojie Guo, "Kindling the darkness: A practical low-light image enhancer," in *Proceedings of the 27th ACM International Conference on Multimedia*, 2019, pp. 1632–1640.
- [23] Xin Tan, Ke Xu, Ying Cao, Yiheng Zhang, Lizhuang Ma, and Rynson W. H. Lau, "Night-time scene parsing with a large real dataset," *IEEE Transactions on Image Processing*, vol. 30, pp. 9085–9098, 2021.
- [24] Fisher Yu, Haofeng Chen, Xin Wang, Wenqi Xian, Yingying Chen, Fangchen Liu, Vashisht Madhavan, and Trevor Darrell, "Bdd100k: A diverse driving dataset for heterogeneous multi-task learning," in *IEEE/CVF Conference on Computer Vision and Pattern Recognition (CVPR)*, June 2020.
- [25] N. Anantrasirichai, J. Burn, and David R. Bull, "Robust texture features based on undecimated dual-tree complex wavelets and local magnitude binary patterns," in *2015 IEEE International Conference on Image Processing (ICIP)*, 2015, pp. 3957–3961.
- [26] Kaiming He, Xiangyu Zhang, Shaoqing Ren, and Jian Sun, "Deep residual learning for image recognition," in *2016 IEEE Conference on Computer Vision and Pattern Recognition (CVPR)*, 2016, pp. 770–778.
- [27] Tsung-Yi Lin, Piotr Dollár, Ross Girshick, Kaiming He, Bharath Hariharan, and Serge Belongie, "Feature pyramid networks for object detection," in *2017 IEEE Conference on Computer Vision and Pattern Recognition (CVPR)*, 2017, pp. 936–944.
- [28] A. Buades, B. Coll, and J.-M. Morel, "A non-local algorithm for image denoising," in *IEEE Computer Society Conference on Computer Vision and Pattern Recognition (CVPR'05)*, 2005, vol. 2, pp. 60–65.
- [29] C. Tomasi and R. Manduchi, "Bilateral filtering for gray and color images," in *Sixth International Conference on Computer Vision (IEEE Cat. No.98CH36271)*, 1998, pp. 839–846.
- [30] Cihang Xie, Yuxin Wu, Laurens van der Maaten, Alan L. Yuille, and Kaiming He, "Feature denoising for improving adversarial robustness," in *The IEEE Conference on Computer Vision and Pattern Recognition (CVPR)*, June 2019.